0026-895X/92/010016-12$03.00/0

MOLECULAR PHARMACOLOGY, 42:16-27

Cloning of Two Mouse Genes Encoding α_2-Adrenergic Receptor Subtypes and Identification of a Single Amino Acid in the Mouse α_2-C10 Homolog Responsible for an Interspecies Variation in Antagonist Binding

RICHARD LINK, DAVID DAUNT, GREG BARSH, ANDRZEJ CHRUSCINSKI, and BRIAN KOBILKA

Howard Hughes Medical Institute (G.B., B.K.), Department of Molecular and Cellular Physiology (R.L., D.D., A.C., B.K.), Division of Cardiovascular Medicine (B.K.), and Department of Pediatrics (G.B.), Stanford University, Stanford, California 94305

Received October 2, 1991; Accepted April 24, 1992

SUMMARY

Molecular cloning and ligand binding studies have shown the α_2 class of adrenergic receptor (α_2-AR) to be a family of at least three related subtypes in humans. These studies have not, however, identified distinct subtype-specific functions for these receptors *in vivo*. It should be possible to extend the analysis of α_2-AR subtype function to the animal level through the use of experimental mammalian embryology in mice. To begin this process, we have isolated two mouse genomic clones encoding α_2-AR subtypes and expressed these genes in COS-7 cells for binding studies. Sequence homology and ligand binding data allow the assignment of one clone (Mα_2-4H) as the mouse homolog of the human α_2-C4 subtype. The other clone (Mα_2-10H) closely resembles the human α_2-C10 subtype in sequence but binds with significantly lower affinity to yohimbine and rauwolscine, members of a distinct class of bulky α_2-selective antagonists commonly used to evaluate α_2-AR function *in vivo*. To define the domain(s) responsible for this unusual binding property, we constructed a series of Mα_2-10H/human α_2-C10 chimeric receptors. Analysis of these receptors identified a conservative Cys^{201} to Ser^{201} change in the fifth transmembrane domain of Mα_2-10H as being responsible for the low affinity of the mouse receptor for yohimbine.

ARs are plasma membrane receptors that mediate the physiological actions of the endogenous catecholamines epinephrine and norepinephrine and are targets for a number of important therapeutic agents. They are members of a diverse family of structurally related receptors that contain seven putative membrane-spanning domains and transduce signals by coupling to heterotrimeric guanine-nucleotide binding proteins. The ARs can be roughly subdivided into three major classes (α_1, α_2, and β), with each class representing a group of related receptor subtypes.

The α_2 class of AR has been implicated in a wide range of physiological processes, including vasomotor regulation, platelet aggregation, analgesia, renal fluid and electrolyte balance, and modulation of norepinephrine release from presynaptic adrenergic nerve terminals (1, 2). These receptors couple primarily to the inhibition of adenylate cyclase and may, to a lesser extent, stimulate polyphosphoinositide hydrolysis (3). Based on the binding of radiolabeled ligands to α_2 receptors in various tissues and cell lines, Bylund *et al.* (4, 5) have subdivided the α_2 class of ARs into a family of three pharmacological subtypes, termed α_2-A, -B and -C. To date, the genes for three human α_2 receptor subtypes have been cloned and localized to different chromosomes (C2, C4, and C10) by somatic cell hybrid analysis (6–8). Homologs of α_2-C2, α_2-C4, and α_2-C10 have been cloned from rat (9–12); in addition, an α_2-C10 homolog has been cloned from pig (13). Expression of these subtype genes in tissue culture cells has demonstrated that they can be differentiated by rank orders of potency for a panel of agonists and antagonists. The human α_2-C10 clone has been assigned to the α_2-A subtype, on the basis of ligand binding and Northern blot analysis (7, 14). Although the human α_2-C2 receptor exhibits α_2-B-like pharmacological properties, the human genomic clone for α_2-C2 did not hybridize with RNA from neonatal rat lung, a rich source of the α_2-B subtype (14). This surprising hybridization result is difficult to understand, because the rat α_2-C2 homolog (RNG-α_2), which shares 82% identity with the human α_2-C2, hybridized strongly to two species (1.3 and 4.0 kb) in neonatal rat lung RNA (11). Despite this inconsistency, Zeng

The first and second authors made equal contributions to this work.

This work was partially funded by the Howard Hughes Medical Institute and Syntex Corp. R.L. was supported by Training Grant 5T32 GM07365 from the National Institute for General Medical Sciences. D.D. was supported by National Institutes of Health Grant 5 RO1 NS28471.

ABBREVIATIONS: AR, adrenergic receptor; SDS, sodium dodecyl sulfate; G protein, guanine nucleotide-binding protein; SSC, standard saline citrate; PCR, polymerase chain reaction; kb, kilobases.

and Lynch (15) have proposed that both the human α_2-C2 and rat RNG-α_2 genes encode the α_2-B subtype. To date, the unambiguous assignment of the human α_2-C4 to one of Bylund's pharmacological subtypes has not been possible. The human α_2-C4 shows pharmacological characteristics consistent with both the α_2-B and α_2-C subtypes (7). Based on RNA hybridization data, Lorenz *et al.* (14) have proposed that the α_2-C4 gene encodes an α_2-B subtype, and they suggested that the α_2-C subtype defined in OKY opossum kidney cells may simply represent an interspecies variation of α_2-C4. In contrast, Zeng and Lynch (15) proposed that both the human α_2-C4 gene and its rat homolog, RG10, encode a distinct α_2-C pharmacological subtype. Clearly, no single classification system for these receptors has received unanimous acceptance.

The synthetic antagonist and agonist compounds used to classify the α_2-ARs into subtypes play no known physiological role *in vivo*. Although the structural features that define the α_2 class may predispose a receptor to bind these ligands, direct selection for a given binding affinity probably does not occur. This line of argument suggests that significant interspecies variation in the binding of these synthetic compounds to the various α_2 subtypes may limit their usefulness as tools for general classification. Therefore, physiological studies that depend on these agents to block or stimulate these receptor subtypes selectively in animal models will be difficult to interpret until the detailed ligand-binding properties of cloned receptors from the animal in question have been defined.

The physiological significance of the multiplicity of α_2-AR genes is an important question that remains unresolved. Individual α_2-AR subtypes have unique patterns of tissue distribution (10, 14, 15), suggesting that they may be functionally distinct. However, when expressed in tissue culture cells, the three human subtypes bind with comparable affinity to the endogenous catecholamines (8). In addition, the human α_2-C4 and α_2-C10 receptors couple to the same G proteins, with only slight differences in efficiency (16). Although these methods have advanced our understanding of α_2-AR function, they have not adequately resolved distinct physiological roles for the three conserved α_2-AR subtype genes.

Modern experimental embryology offers a powerful alternative approach to probing the physiological significance of α_2-AR diversity *in vivo*. Recent advances in the manipulation of mammalian embryos would allow the expression of specific α_2-AR subtype genes to be altered in mice (17–19). These techniques, however, require a detailed knowledge of the endogenous mouse α_2-AR genes. To this end, we have sought to identify and clone genes encoding mouse α_2-AR subtypes.

Here we present the nucleotide sequence and pharmacological characterization of genomic clones encoding mouse homologs of the human α_2-C4 and α_2-C10 receptors (Mα_2-4H and Mα_2-10H, respectively). In addition, through the construction of chimeric mouse/human receptors, we have identified Ser^{201} in the fifth transmembrane domain of Mα_2-10H as being responsible for an interspecies variation in antagonist binding.

Materials and Methods

Cloning and DNA Sequencing

^{32}P-labeled probes were synthesized from the human platelet α_2-AR genomic clone (α_2-C10; 0.95-kb *Pst*I fragment and from the human kidney cDNA encoding α_2-C4 (1.0-kb *Nco*I/*Sma*I fragment) (7) by random priming, followed by purification on a Sephadex G-50 column. These probes were used to screen a mouse 129/Sv embryonic stem cell genomic library in EMBL-3 (provided by H. Roelink, Howard Hughes Medical Institute at Columbia University). Duplicate nylon filters (Magnagraph; Micron Separations Inc., Westboro, MA) were hybridized in a solution containing 5× SSC (0.75 M sodium chloride, 0.075 M sodium citrate, pH 7.0), 5× Denhardt's solution [0.1% (w/v) Ficoll, 0.1% (w/v) polyvinylpyrrolidone, 0.1% (w/v) bovine serum albumin], 0.05 M sodium phosphate (pH 7.0), 0.1% sodium pyrophosphate, 25 μg/ml sheared salmon sperm DNA, 0.1% (w/v) SDS, 50% formamide, and ^{32}P-labeled probe (1×10^6 cpm/ml), at 42°, for 18–22 hr. After hybridization, filters were washed three times at 60° in 1× SSC (0.15 M sodium chloride, 0.015 M sodium citrate, pH 7.0), 0.1% SDS, for 45 min. The clones corresponding to the human α_2-C10 and α_2-C4 could be differentiated by washing for 45 min at 65° in 0.1× SSC (0.015 M sodium chloride, 0.0015 M sodium citrate, pH 7.0). λ phage hybridizing to the various probes were plaque purified, and λ DNA was prepared. For Southern blot analysis and subcloning, a 10.5-kb *Sal*I fragment from phage 22, which hybridized to the human C10 probe (clone Mα_2-10H), and a 6.5-kb *Eco*RI fragment from phage 13, which hybridized to the human C4 probe (clone Mα_2-4H), were subcloned into the corresponding polylinker sites of Bluescript SK− (Stratagene Cloning Systems, La Jolla, CA). Progressive unidirectional deletions were prepared for sequencing with the Erase-A-Base kit (Promega Corporation, Madison, WI). Nucleotide sequencing of both strands was performed by the Sanger dideoxynucleotide chain termination method (20), by primer extension with T7 DNA polymerase on double-stranded DNA templates (Sequenase version 2.0; United States Biochemicals, Cleveland, OH). After the termination reaction and before addition of stop solution, samples were treated with terminal transferase (Stratagene) for 30 min (21). Sequence compression artifacts were resolved by the substitution of dITP for dGTP in the sequencing protocol. Alignment analysis of protein and nucleic acid sequences was carried out using the GCG-BESTFIT program, with a gap weight of 3.0 and a gap length weight of 0.1 (22, 23), (Genetics Computer Group, Inc.).

Southern Analysis

Ten micrograms of BALB/c mouse genomic DNA were digested to completion with either *Bam*HI, *Eco*RI, *Pst*I, or *Hind*III and were separated on a 1% agarose gel. The DNA was depurinated by treatment twice for 20 min in 100 mM HCl, denatured in 0.5 N NaOH/1.5 M NaCl for 45 min, neutralized in 0.5 M Tris·HCl (pH 7.4)/1.5 M NaCl for 45 min, and transferred to a nylon membrane (Magnagraph; Micron Separations Inc.) in a solution of 20× SSC. DNA was covalently bonded to the membrane by UV irradiation and hybridized to ^{32}P-labeled mouse and human DNA probes, as described previously. The human probes were described above. The mouse probe used was either a 1.1-kb *Nco*I/*Xmn*I fragment from Mα_2-10H or a 1.6-kb *Nco*I/*Bam*HI fragment from Mα_2-4H. Blots hybridized to the human probes were washed at low stringency (1× SSC, 0.1% SDS; 60° for 40 min). Blots hybridized to the mouse probes were washed at high stringency (0.2× SSC, 0.1% SDS; 60° for 40 min).

Expression

Eukaryotic expression vectors containing the human α_2-C4 and α_2-C10 coding sequences (pBC-Hα_2-C4 and pBC-Hα_2-C10) were prepared by cloning into pBC12BI (24), as previously described (7). The expression vectors for the mouse α_2-AR clones were prepared as follows. A version of pBC12BI containing the β_2-AR was opened by digestion with *Nco*I and *Bam*HI. The β_2-AR coding sequence was replaced with either a 1.6-kb *Nco*I/*Bam*HI fragment from Mα_2-4H (pBC-Mα_2-4H) or a 4.9-kb *Nco*I/*Bam*HI fragment from Mα_2-10H (pBC-Mα_2-10H). Both human and mouse α_2-AR clones were transiently expressed in COS-7 cells, using a DEAE-dextran transfection protocol (25).

Construction of Chimeric Mouse Mα_2-10H/Human α_2-C10 Receptors

Chimera 1. A 2.3-kb *Xmn*I fragment of the human α_2-C10 receptor (from pBC-Hα_2-C10) containing transmembrane domains TM_{6-7} and

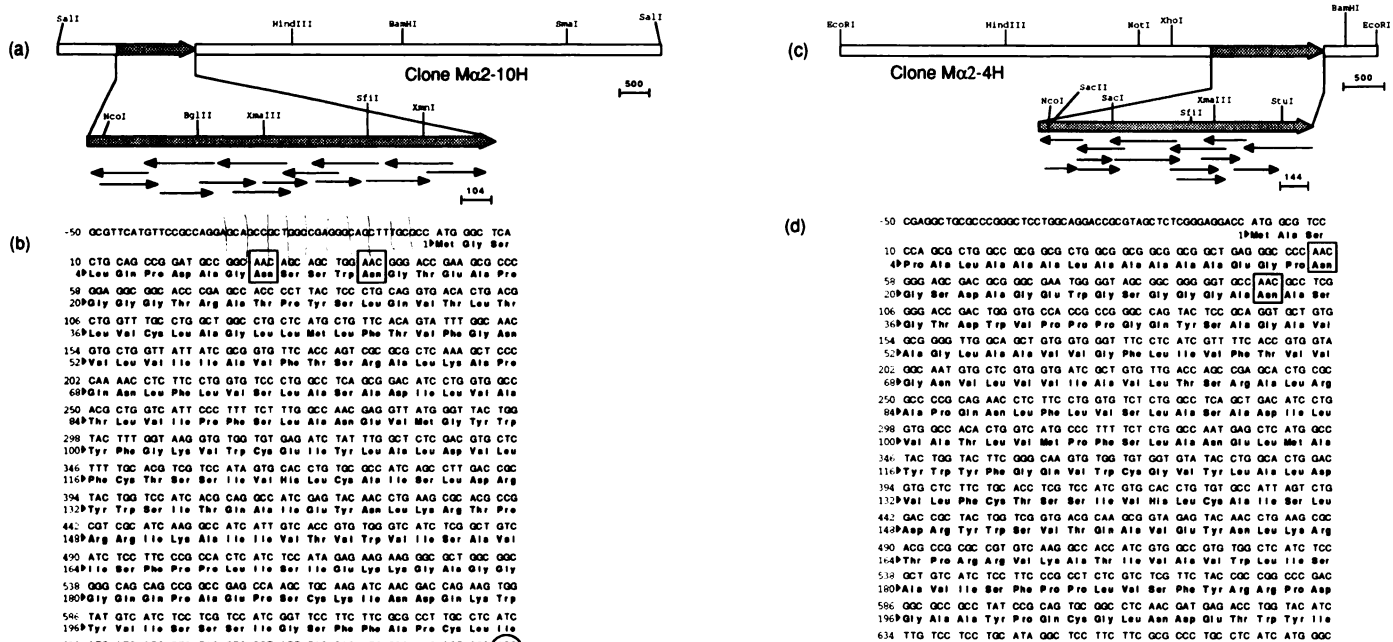

Fig. 1. Sequencing strategy, nucleotide sequence, and deduced amino acid sequence of the mouse α_2-AR clones Mα_2-10H and Mα_2-4H. a, Restriction map for clone Mα_2-10H and the strategy for sequencing via exonuclease III deletions and synthetic oligonucleotide primers. b, Nucleotide and deduced amino acid sequences for clone Mα_2-10H. c, Restriction map for clone Mα_2-4H and the strategy for sequencing. d, Nucleotide and deduced amino acid sequences for clone Mα_2-4H. *Hatched boxes*, coding region, with the *arrowhead* pointing in the sense direction. *Small arrows*, direction and extent of sequencing. *Squares*, potential sites for *N*-linked glycosylation; *circles*, threonines within consensus sites for phosphorylation by cAMP-dependent protein kinase; *underlining*, potential ATP/GTP-binding domain in clone mα_2-10H.

the carboxyl-terminal tail was spliced into the mouse Mα_2-10H clone at the *Xmn*I site. This produced a chimeric receptor (pMHCR1) composed of mouse sequence from the amino terminus to the end of the third cytoplasmic loop (mouse Met^1 to Arg^{371}) and human sequence encoding TM_{6-7} and the carboxyl terminus (human Phe^{372} to Val^{450}) (see Fig. 6).

Chimera 2. To construct pMHCR2, a three-fragment ligation was carried out with the following three fragments: 1) a 4.2-kb *Bgl*II/*Sal*I fragment from chimera 1 containing the amino terminus, TM_{1-2}, and the first extracellular loop of mouse clone Mα_2-10H (mouse Met^1 to Glu^{107}); 2) a 0.8-kb *Bgl*II/*Xmn*I fragment from the human α_2-C10 expression vector (pBC-Hα_2-C10) containing TM_{3-5} and the third cytoplasmic loop (human Ile^{108} to Arg^{371}); and 3) a 0.4-kb *Xmn*I/*Sal*I fragment containing TM_{6-7} and the carboxyl tail from the mouse receptor clone Mα_2-10H (mouse Phe^{372} to Val^{450}; see Fig. 6).

Chimera 3. Plasmid p141B was constructed by subcloning a 1.65-kb *Sac*I fragment containing the entire coding sequence of Mα_2-10H into the *Sac*I site of Bluescript SK−. A unique *Bam*HI site was engineered, with the PCR, immediately following the termination codon. Plasmid pC10/C4/RV1 was constructed by digestion with *Bam*HI and recircularization to remove all the 3′ untranslated sequence in p141B. This process removed an *Acc*I site located in the 3′ untranslated region, of the Mα_2-10H gene. Chimera 3 (pMHCR3) was constructed by ligating a 0.76-kb *Acc*I/*Sal*I fragment from pC10/C4/RV1 into the *Acc*I/*Sal*I sites of pMHCR2. This receptor contains Mα_2-10H sequence encoding the amino terminus, TM_{1-2}, and the first extracellular loop (mouse Met^1 to Glu^{107}), human α_2-C10 sequence encoding TM_{3-5} (human Ile^{108} to Val^{215}), and Mα_2-10H sequence encoding the third cytoplasmic loop through the carboxyl terminus (mouse Tyr^{216} to Val^{450}).

Mα_2-10H$^{(Cys^{201})}$. Plasmid pC10/C4/RV1 was digested with *Bam*HI, filled in with Klenow fragment, and digested with *Nco*I. Plasmid p234 was constructed by ligating this 1.6-kb *Nco*I/blunt fragment into a 2.1-kb *Nco*I/*Sal*I vector from pMHCR1 (the *Sal*I site was filled in with Klenow). p234 represents a wild-type mouse Mα_2-10H receptor, in which the *Acc*I and *Sal*I sites 3′ to the coding sequence have been removed. To construct Mα_2-10H$^{(Cys^{201})}$, PCR was used to mutate the

mouse residue at position 201 (serine; codon, TCC) to the corresponding residue in the human α_2-C10 (cysteine; codon, TGC). Mα_2-10H$^{(Cys^{201})}$ contains entirely mouse Mα_2-10H sequence, except for this single point mutation.

Binding Assays

Membranes were prepared from COS-7 cells 3 days after transfection, as described previously (25). Binding experiments were performed in a 500-μl volume in 75 mM Tris, 12.5 mM $MgCl_2$, 1 mM EDTA, pH 7.4, and incubated for 90 min at room temperature. The bound radioactivity was separated from free by vacuum filtration through GF/C filter paper, at 5°. Saturation isotherms were performed by incubating the membranes with varying concentrations of [^{3}H]yohimbine (72.3 Ci/mmol; New England Nuclear DuPont, Wilmington, DE) or [^{3}H] atipamezole (50.0 Ci/mmol; Farmos Ltd., Orion, Corp., Turku, Finland). Nonspecific binding was determined by adding 100 μM yohimbine to radiolabeled binding studies. Competition experiments were carried out by incubating membranes with varying concentrations of competing ligand and 2 nM [^{3}H]yohimbine (for human α_2-C4 and α_2-C10 and mouse α_2-C4) or 0.5 nM [^{3}H]atipamezole (for mouse α_2-C10). Nonspecific binding was determined in the presence of 100 μM yohimbine. Equilibrium dissociation constants were determined from saturation isotherms and competition curves. Saturation isotherm data were analyzed by a nonlinear least-squares curve-fitting technique, and the competition data were analyzed according to a four-parameter logistic equation, to determine K_d and EC_{50} values, using GraphPAD software (GraphPAD Software Inc., San Diego, CA).

Results

Isolation of mouse genomic clones. A mouse genomic library in EMBL3 was screened with the human α_2-C4 and α_2-C10 probes described in Materials and Methods. Low stringency hybridization (5× SSC, 42°; wash, 1× SSC, 60°) allowed the isolation of three unique clones (each containing an insert of >17 kb), based on restriction analysis. Restriction fragments from the three clones were selected and subcloned into Bluescript SK− for further analysis. Two of these fragments were later shown to represent independent isolates of one mouse gene, Mα_2-10H; the third was shown to represent another gene, Mα_2-4H.

To determine the copy number of the mouse α_2-AR clones, we compared the pattern of mouse genomic fragments detected by our cloned mouse fragments at high stringency (Fig. 2 b and c) with the pattern detected by the human α_2-C10 probe at low stringency (Fig. 2a). Cross-species hybridization with the human α_2-C10 probe detected 0.5-, 1.4-, 3.0-, and 5.1-kb *Pst*I, 5.8-kb *Hind*III, 5.5- and 9.8-kb *Eco*RI, and 2.4- and 5.5-kb *Bam*HI fragments. The 5.1-kb *Pst*I and 9.8-kb *Eco*RI fragments represent the endogenous mouse Mα_2-10H gene; the 3.0-kb *Pst*I and 5.5-kb *Eco*RI fragments represent the endogenous mouse Mα_2-4H gene. The mouse probes recognized a single fragment in all the lanes at high stringency, suggesting that Mα_2-4H and Mα_2-10H represent genes present as single copies in the murine genome. The 2.4-kb *Bam*HI fragment recognized by the human α_2-C10 probe at low stringency did not hybridize with either of the mouse genes at high stringency. Subsequent hybridization of this blot with a 900-base pair PCR product derived from the human α_2-C2 gene (provided by J. Lomasney and R. J. Lefkowitz, Howard Hughes Medical Institute at Duke University) suggests that the 2.4-kb *Bam*HI fragment represents the mouse homolog to human α_2-C2 (data not shown).

Comparison of deduced amino acid sequences. A 5.0-kb *Nco*I/*Bam*HI fragment of Mα_2-10H contained an open reading frame of 1350 bases, encoding a protein of 450 amino acids (Fig. 1, a and b). A 1.6-kb *Nco*I/*Bam*HI fragment of Mα_2-4H contained an open reading frame of 1374 bases, encoding a protein of 458 amino acids (Fig. 1, c and d). In both cases, the first translated ATG was selected, based on homology both to the published human α_2-AR sequences (6, 7) and to the Kozak consensus sequence for translational initiation (26).

Hydropathy analysis of Mα_2-10H and Mα_2-4H (data not shown) indicates that they may conform to the previously postulated structural model for the ARs (27). In this model, which is based on extrapolations from the structure of bacterial rhodopsin (28), seven hydrophobic stretches of amino acids serve as membrane-spanning domains. The homology between the two mouse clones is highest in these putative transmembrane domains (Figs. 3 and 4). Receptor clones Mα_2-10H and Mα_2-4H exhibited 58% identity in amino acid sequence overall, consistent with published comparisons between α_2-AR subtype genes from other species [human α_2-C10/α_2-C4, 55% (7); rat RG20/RG10, 56% (9)]. Both receptors have three potential sites for *N*-linked glycosylation (Asn-X-Ser/Thr) (two at the amino terminus and one buried within TM_7).

The protein encoded by Mα_2-4H (Fig. 3) exhibited 99% identity to the rat α_2-C4 homolog (RG10), 89% identity to the human α_2-C4, 59% to the porcine α_2-C10 homolog, 58% to the human α_2-C10, 56% to the rat α_2-C10 homolog (RG20), 55% to the rat α_2-C2 homolog (RNG-α_2-AR) (11), and 54% to the human α_2-C2. Based on sequence homology and ligand binding data (see below), this receptor appears to be the mouse counterpart to the human α_2-C4 and its rat homolog, RG10. When the mouse receptor is compared with the human α_2-C4, the majority of the differences are found in the amino terminus and third cytoplasmic loop (Fig. 3). Only four changes are found in the transmembrane domains, as defined by Regan *et al.* (7). The mouse receptor is two residues shorter than the human protein, due to a two-amino acid deletion in the third cytoplasmic loop. In addition, Mα_2-4H shares with its human homolog a single consensus site in the third cytoplasmic loop (Arg/Lys-Arg/Lys-X-Ser/Thr; Thr^{377}) for phosphorylation by c-AMP-dependent protein kinase.

The protein encoded by Mα_2-10H exhibited 96% identity to the rat α_2-C10 homolog (RG20), 92% to the human α_2-C10, 92% to the porcine α_2-C10 homolog, 58% to the rat α_2-C4 homolog (RG10), 56% to the human α_2-C2, 55% to the human α_2-C4, and 54% to the rat α_2-C2 homolog (RNG-α_2-AR). Based on the high degree of sequence homology to the rat RG20 receptor and some unusual antagonist binding properties in common with RG20 (see below), the mouse Mα_2-10H clone appears to be the mouse homolog of the rat RG20. In addition, we believe that Mα_2-10H represents the mouse species homolog of the human α_2-C10 receptor (see Discussion). When compared with the human receptor, the majority of the changes exist in the third cytoplasmic loop, although seven differences are found in the transmembrane domains. Mα_2-10H contains two consensus sites (Thr^{227} and Thr^{373}) for c-AMP-dependent phosphorylation, both in the third cytoplasmic loop. In addition, the mouse Mα_2-10H clone contains a single consensus ATP/GTP-binding site motif (Gly^{314}-Thr^{321}) in the third cytoplasmic loop. This so-called "A" consensus sequence (Ala/Gly-X-X-X-X-Gly-Lys-Ser/Thr) can be found in a wide variety of different ATP- and GTP-binding proteins, including ATP synthase,

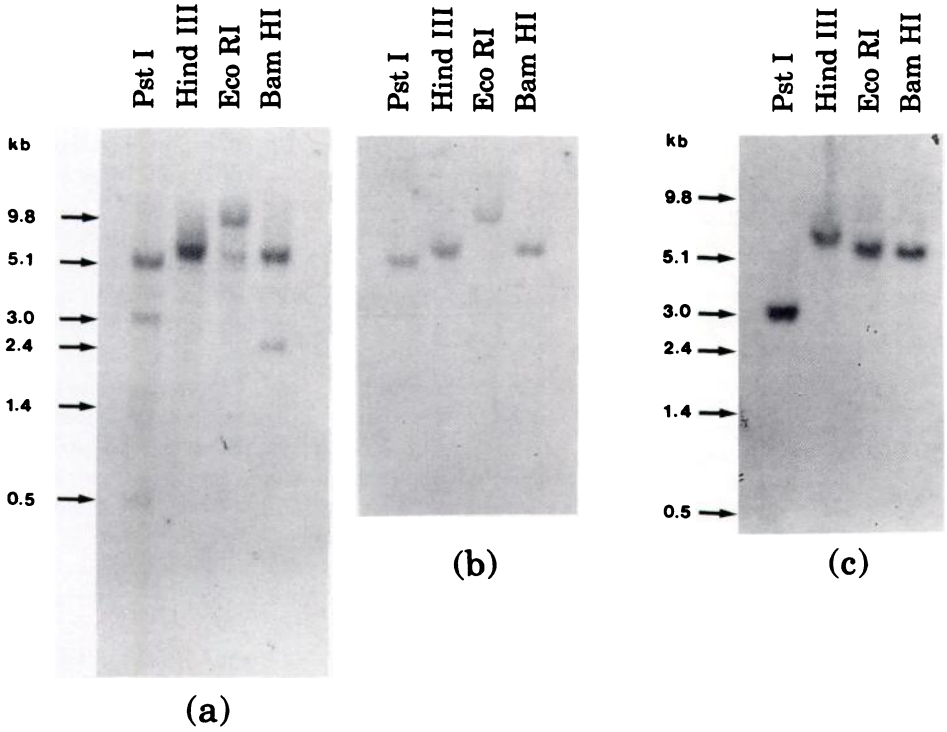

Fig. 2. Southern analysis of mouse genomic DNA hybridized with mouse or human α_2-AR probes. a, Low stringency hybridization with a 0.95-kb *PstI* fragment from the human α_2-C10 gene (see Materials and Methods); b, high stringency hybridization with a 1.1-kb *NcoI/XmnI* fragment from mouse clone Mα_2-10H; c, high stringency hybridization with a 1.6-kb *NcoI/BamHI* fragment from mouse clone Mα_2-4H. Restriction enzymes used for digestion of genomic DNA and sizes of bands are as marked. a and b, Two independent probings of the same blot. The molecular sizes shown are in kb.

myosin heavy chain, and the α-subunits of heterotrimeric G proteins (29).

Expression and ligand binding studies. The two mouse clones (Mα_2-10H and Mα_2-4H) were subcloned into the eukaryotic expression vector pBC12BI and transiently expressed in COS-7 cells. Equilibrium dissociation constants (either K_d or K_i) for several α_2-AR agonists and antagonists are given in Table 1. Representative saturation curves for the mouse clones Mα_2-10H and Mα_2-4H are included (Fig. 5) for both yohimbine and atipamezole, along with their molecular structures. Binding studies were done simultaneously on mouse and human α_2-ARs expressed in COS-7 cells, to facilitate comparison between the mouse and human receptor subtypes.

The mouse receptor encoded by clone Mα_2-4H exhibited binding affinity very similar to that of the human α_2-C4 for all antagonists and agonists tested (Table 1; Fig. 5b). These data, combined with the strong degree of sequence homology, support the definition of Mα_2-4H as the mouse homolog of the human α_2-C4 receptor subtype. The affinity of the various ligands for human α_2-C4, in our hands, was comparable to previously published results (7). Atipamezole, a high affinity α_2-selective antagonist (30), was also screened, because its structure differs significantly from the class of bulky antagonists that includes yohimbine and its diastereomer, rauwolscine (Fig. 5).

Although the protein encoded by mouse clone Mα_2-10H exhibited 92% homology to human α_2-C10, its pharmacological profile differed from that of human α_2-C10 in one major aspect. The α_2-selective antagonist yohimbine, which does not display subtype selectivity for the human α_2-ARs, bound with a significantly lower affinity (K_i = 53.6 nM) to mouse clone Mα_2-10H than to clone Mα_2-4H (K_d = 3.8 nM) or either of the human receptor subtypes (α_2-C10, K_d = 3.4 nM; α_2-C4, K_d = 3.1 nM; see Fig. 5). A similar binding profile has been observed in the rat, where the RG20 receptor (a receptor most closely homologous to the human α_2-C10) binds yohimbine with an affinity of 61 nM (9). Rauwolscine, a diastereomer of yohimbine, also bound with lower affinity to the mouse Mα_2-10H clone (K_i = 53.3 nM) than the human α_2-C10 (K_i = 4.6 nM). In contrast, the antagonist atipamezole bound with high affinity to all mouse and human α_2-ARs screened. Both yohimbine and rauwolscine belong to a class of polycyclic ligands with a rigid L-shape, whereas atipamezole has a smaller, potentially more flexible structure (Fig. 5). Because of the low affinity of Mα_2-10H for yohimbine, [^{3}H]atipamazole was used for all competition assays with clone Mα_2-10H. Competition data generated using this ligand were comparable to results with [^{3}H]yohimbine (data not shown). Prazosin, an antagonist whose affinity differs between the human receptor subtypes (α_2-C4, K_i = 121.1 nM; α_2-C10, K_i = 2034 nM), also showed a higher affinity for the mouse α_2-C4 homolog (Mα_2-4H) (K_i = 97.3 nM) than the mouse α_2-C10 homolog (Mα_2-10H) (K_i = 2157 nM). In addition, the mouse Mα_2-10H exhibited a slightly lower affinity for WB-4101 (K_i = 261.2 nM), an antagonist that binds to both the human receptors with high affinity (α_2-C4, K_i = 4.6 nM; α_2-C10, K_i = 7.8 nM) Finally, Mα_2-10H bound all the agonists tested with affinities similar to those of the human α_2-C10.

Both the human α_2-C10 and porcine α_2-C10 homolog bound to yohimbine with high affinity (human, K_d = 3.4 nM; porcine, EC_{50} = 7.5 nM) (13), whereas the rodent α_2-C10 homologs exhibited an affinity almost 20-fold lower [rat RG20, K_i = 61 nM (9); mouse Mα_2-10H, K_i = 53.6 nM]. It should be possible to identify key "candidate" residues common to both rodent receptors yet different from the human and porcine sequences, which might result in low affinity for this class of antagonists. In Fig. 4, these candidate residues are highlighted. Only four candidate residues are found within the putative transmembrane domains, as defined by Guyer *et al.* (13).

Expression and ligand binding of chimeric receptors. We were interested in identifying domains in the mouse Mα_2-10H receptor that might be responsible for its low affinity for yohimbine. To accomplish this, four recombinant mouse (Mα_2-10H)/human (α_2-C10) chimeric receptors were constructed

```
                1                                                  50
HumanA2C4   MASPALAAAL AVAAAAGPNA SGAGERGSGG VANASGASWG PPRGQYSAGA
  RatRG10   MASPALAAAL AAAAAEGPNG SDAGEWGSGG GANASGTDWG PPPGQYSAGA
   MA2-4H   MASPALAAAL AAAAAEGPNG SDAGEWGSGG GANASGTDWV PPPGQYSAGA

CONSENSUS  MASPALAAAL AaAAAeGPNg SdAGEwGSGG gANASGtdWg PPpGQYSAGA

                51                                                 100
HumanA2C4   VAGLAAVVGF LIVFTVVGNV LVVIAVLTSR ALRAPQNLFL VSLASADILV
  RatRG10   VAGLAAVVGF LIVFTVVGNV LVVIAVLTSR ALRAPQNLFL VSLASADILV
   MA2-4H   VAGLAAVVGF LIVFTVVGNV LVVIAVLTSR ALRAPQNLFL VSLASADILV

CONSENSUS  VAGLAAVVGF LIVFTVVGNV LVVIAVLTSR ALRAPQNLFL VSLASADILV
                      TM #1

              101                                                 150
HumanA2C4   ATLVMPFSLA NELMAYWYFG QVWCGVYLAL DVLFCTSSIV HLCAISLDRY
  RatRG10   ATLVMPFSLA NELMAYWYFG QVWCGVYLAL DVLFCTSSIV HLCAISLDRY
   MA2-4H   ATLVMPFSLA NELMAYWYFG QVWCGVYLAL DVLFCTSSIV HLCAISLDRY

CONSENSUS  ATLVMPFSLA NELMAYWYFG QVWCGVYLAL DVLFCTSSIV HLCAISLDRY
              TM #2                                  TM #3

              151                                                 200
HumanA2C4   WSVTQAVEYN LKRTPRRVKA TIVAVWLISA VISFPPLVSL YRQPDGAAYP
  RatRG10   WSVTQAVEYN LKRTPRRVKA TIVAVWLISA VISFPPLVSF YRRPDGAAYP
   MA2-4H   WSVTQAVEYN LKRTPRRVKA TIVAVWLISA VISFPPLVSF YRRPDGAAYP

CONSENSUS  WSVTQAVEYN LKRTPRRVKA TIVAVWLISA VISFPPLVSf YRrPDGAAYP
                                          TM #4

              201                                                 250
HumanA2C4   QCGLNDETWY ILSSCIGSFF APCLIMGLVY ARIYRVAKRR TRTLSEKRAP
  RatRG10   QCGLNDETWY ILSSCIGSFF APCLIMGLVY ARIYRVAKLR TRTLSEKRGP
   MA2-4H   QCGLNDETWY ILSSCIGSFF APCLIMGLVY ARIYRVAKLR TRTLSEKRGP

CONSENSUS  QCGLNDETWY ILSSCIGSFF APCLIMGLVY ARIYRVAKlR TRTLSEKRgP
                              TM #5

              251                                                 300
HumanA2C4   VGPDGASPTT ENGLGAAAGE ARTGTARPRP PTWSRTRAAQ RPRGGAPGPL
  RatRG10   ARPDGASPTT ENGLGKAAGE NGHCAPPRTE VEPDESSAAE RRR..RRGAV
   MA2-4H   AGPDGASPTT ENGLGKAAGE NGHCAPPRTE VEPDESSAAE RRR..RRGAL

CONSENSUS  agPDGASPTT ENGLGkAAGE nghcapprte vepdessAAe RrR..rrGal

              301                                                 350
HumanA2C4   RRGGRRRAGA EGGAGGADGQ GAGPGAAQSG ALTASRSPGP GGRLSRASSR
  RatRG10   RRGGRRREGA EGDTGSADGP GPGLAAEQ.G ARTASRSPGP GGRLSRASSR
   MA2-4H   RRGGRRREGA EGDTGSADGP GPGLAAEQ.G ARTASRSPGP GGRLSRASSR

CONSENSUS  RRGGRRReGA EGdtGsADGp GpGlaAeQ.G ArTASRSPGP GGRLSRASSR

              351                                                 400
HumanA2C4   SVEFFLSRRR RARSSVCRRK VAQAREKRFT FVLAVVMGVF VLCWFPFFFI
  RatRG10   SVEFFLSRRR RARSSVCRRK VAQAREKRFT FVLAVVMGVF VLCWFPFFFS
   MA2-4H   SVEFFLSRRR RARSSVCRRK VAQAREKRFT FVLAVVMGVF VLCWFPFFFS

CONSENSUS  SVEFFLSRRR RARSSVCRRK VAQAREKRFT FVLAVVMGVF VLCWFPFFFs
                                                    TM #6

              401                                                 450
HumanA2C4   YSLYGICREA CQVPGPLFKF FFWIGYCNSS LNPVIYTVFN QDFRPSFKHI
  RatRG10   YSLYGICREA CQLPEPLFKF FFWIGYCNSS LNPVIYTVFN QDFRRSFKHI
   MA2-4H   YSLYGICREA CQLPEPLFKF FFWIGYCNSS LNPVIYTVFN QDFRRSFKHI

CONSENSUS  YSLYGICREA CQlPePLFKF FFWIGYCNSS LNPVIYTVFN QDFRrSFKHI
                                          TM #7

              451         461
HumanA2C4   LFRRRRRGFR Q*
  RatRG10   LFRRRRRGFR Q*
   MA2-4H   LFRRRRRGFR Q*

CONSENSUS  LFRRRRRGFR Q*
```

Fig. 3. Sequence comparison of the mouse Mα_2-4H receptor with the human α_2-C4 (7) and rat α_2-C4 homolog (RG10) (9). Amino acid sequences (one-letter codes) were pairwise aligned using the GCG-BESTFIT and GCG-LINEUP programs (as described in Materials and Methods). *Underlining*, the seven putative transmembrane domains [TM_{1-7}, as defined by Regan *et al.* (7)]. A consensus sequence is included in which *upper case letters* denote a residue found in all the receptors, *lower case letters* denote a residue found in two of three receptors, and a *period* denotes a residue not found in more than one receptor.

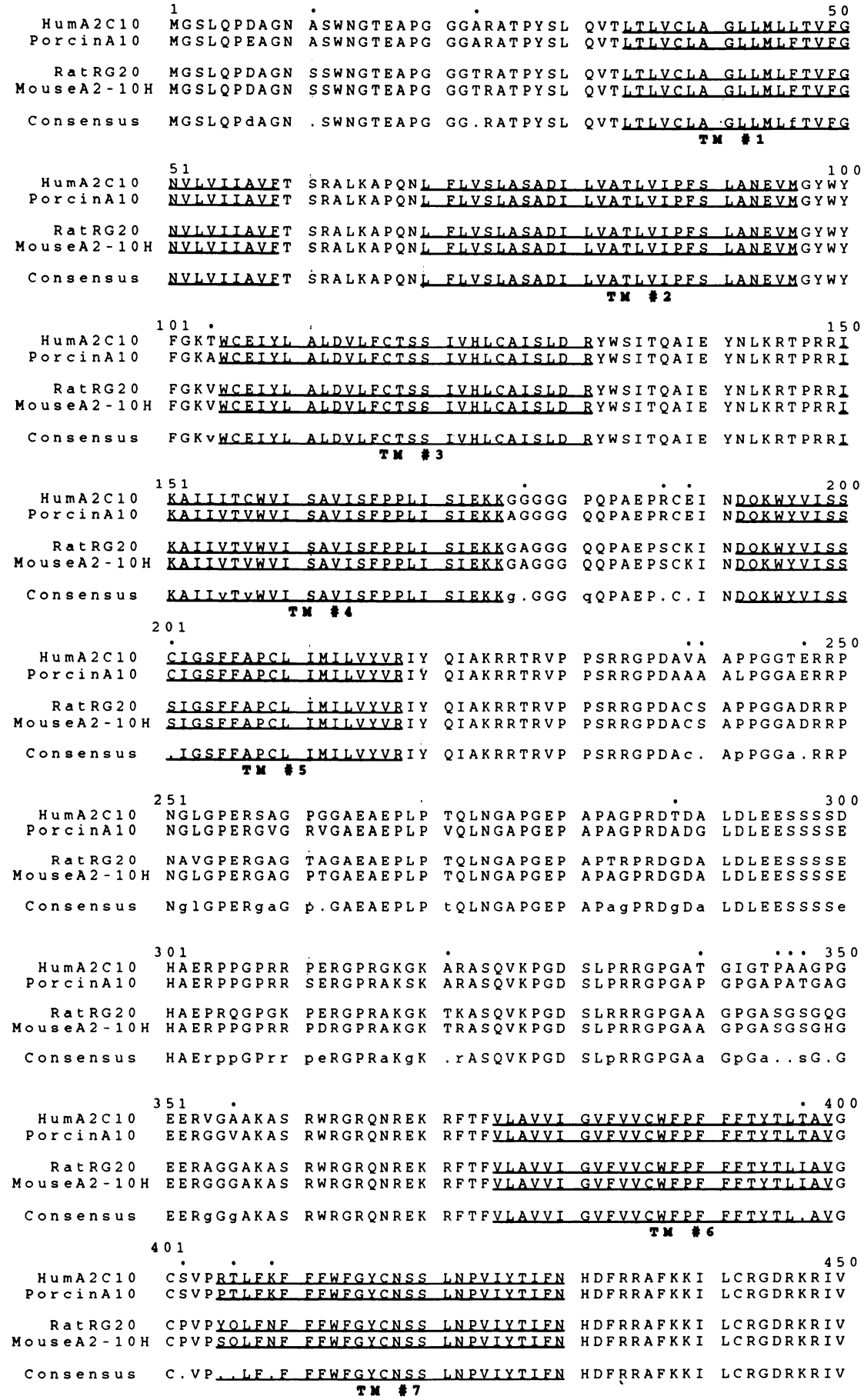

Fig. 4. Sequence comparison of the mouse Mα_2-10H receptor with the human α_2-C10 (6), porcine α_2-C10 (13), and rat RG10 (9) receptors. Amino acid sequences (one-letter codes) were pairwise aligned using the GCG-BESTFIT and GCG-LINEUP programs (as described in Materials and Methods). *Underlining*, the seven putative transmembrane domains [TM_{1-7}, as defined by Guyer *et al.* (13)]. ·, Candidate residues potentially responsible for the low yohimbine binding affinity observed for the rodent receptors (see Results). A consensus sequence is included in which *upper case letters* denote residues found in all the receptors and *lower case letters* denote residues found in two or more receptors. A *period* denotes a residue not found in more than one receptor.

TABLE 1

Equilibrium dissociation constants of various AR ligands for human and mouse α_2-AR subtypes and mouse (Mα_2-10H)/human (α_2-C10) chimeric receptors expressed in COS-7 cells

Binding assays were performed as described in Materials and Methods. Equilibrium dissociation constants that are marked are K_d; all others are K_i. Values represent an average of three independent binding assays. Human and mouse receptor subtypes were assayed simultaneously, for comparison purposes.

	K_i (or K_d)							
	Human α_2-C4	Mouse Mα_2-4H	Human α_2-C10	Mouse Mα_2-10H	MHCR1	MHCR2	MHCR3	Mα_2-10H$^{(Cys^{201})}$
	nM							
Antagonists								
Atipamezole	3.6 ± 0.4	1.6 ± 0.02	2.9 ± 0.2	0.86 ± 0.20[a]	1.3 ± 0.2[a]	8.4 ± 1.3[a]	ND[b]	ND
Yohimbine	3.1 ± 0.1[a]	3.8 ± 0.8[a]	3.4 ± 0.6[a]	53.6 ± 7.3	37.0 ± 1.0[a]	8.4 ± 0.5[a]	4.8 ± 0.2[a]	10.8 ± 0.9[a]
Rauwolscine	1.7 ± 0.2	0.8 ± 0.1	4.6 ± 0.7	53.3 ± 4.1	ND	ND	ND	ND
Prazosin	121.1 ± 10.4	97.3 ± 17.7	2034 ± 350.4	2157 ± 216.0	ND	ND	ND	ND
WB-4101	4.6 ± 0.7	7.8 ± 2.5	22.7 ± 1.8	261.2 ± 17.9	ND	ND	ND	ND
Idazoxan	52.3 ± 7.7	9.8 ± 0.7	12.2 ± 3.7	9.5 ± 1.9	ND	ND	ND	ND
Agonists								
Dexmedetomidine	8.4 ± 0.8	7.2 ± 0.4	8.8 ± 0.2	11.8 ± 0.6	ND	ND	ND	ND
p-Aminoclonidine	204 ± 24.8	102 ± 15.5	77.4 ± 7.2	76.8 ± 10.2	ND	ND	ND	ND
(−)-Norepinephrine	342 ± 75.2	648 ± 90.2	2471 ± 546.7	5759 ± 550.8	ND	ND	ND	ND
(−)-Epinephrine	218 ± 17.7	494 ± 10.9	1170 ± 145.5	2512 ± 160.2	ND	ND	ND	ND
Oxymetazoline	205.9 ± 38.9	108.6 ± 22.1	12.8 ± 3.8	32.6 ± 1.4	ND	ND	ND	ND

[a] K_d.
[b] ND, not done.

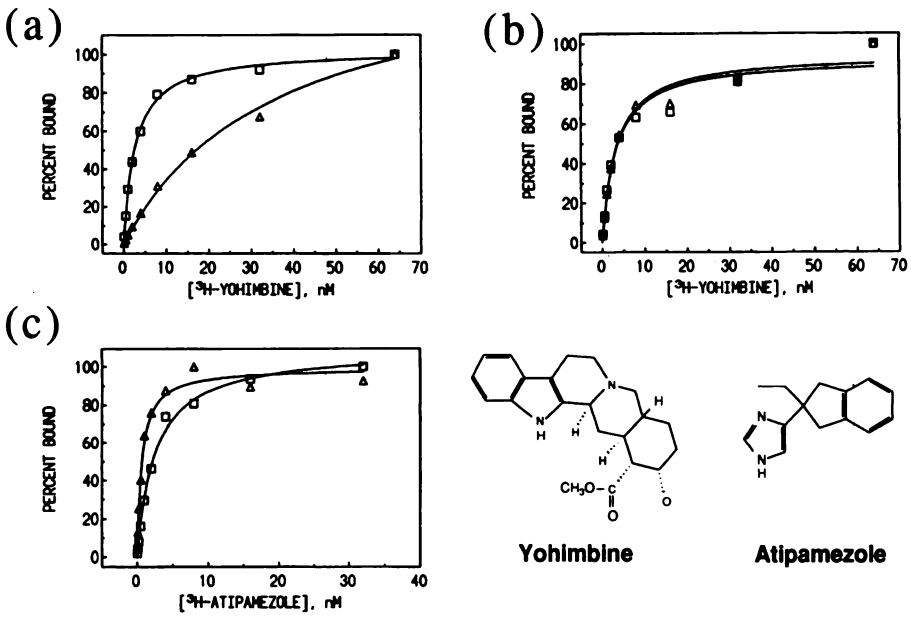

Fig. 5. Representative yohimbine and atipamezole saturation curves for mouse and human α_2-AR subtypes. a, Yohimbine saturation curve for the mouse Mα_2-10H (△) and human α_2-C10 (□) receptors. b, Yohimbine saturation curve for the mouse Mα_2-4H (△) and human α_2-C4 (□) receptors. c, Atipamezole saturation curve for the mouse Mα_2-10H (△) and human α_2-C10 (□) receptors. In all cases, both receptors on each graph were assayed simultaneously. The structures of yohimbine and atipamezole are included for reference.

(Fig. 6), expressed in COS-7 cells, and analyzed by binding assays (Table 1).

Chimera 1 (MHCR1) consists of a mouse Mα_2-10H receptor in which five residues have been changed to their corresponding residues in the human α_2-C10 (one in TM_6, one in extracellular loop EL_3, and three in TM_7). All the residues were candidate residues, as defined above. This receptor bound atipamezole with an affinity comparable to that of both the mouse and human receptors (K_d = 1.3 nM) but did not show an appreciably higher affinity for yohimbine than did the wild-type mouse receptor (K_d = 37 nM).

Chimera 2 (MHCR2) is a mouse Mα_2-10H receptor in which 27 individual residues have been changed to their human counterparts, although only 14 fit the category of candidate residues (three in EL_2, one in TM_5, and 10 in cytoplasmic loop CL_3). This receptor bound yohimbine (K_d = 8.4 nM) with an affinity much more similar to that of the human α_2-C10, suggesting that one or more of the 14 candidate residues replaced is responsible for the low affinity of the wild-type mouse receptor for yohimbine. Interestingly, this chimera bound atipamezole with an affinity 10-fold lower than that of the wild-type Mα_2-10H receptor (MHCR2, K_d = 8.4 nM; wild-type Mα_2-10H, K_d = 0.86 nM). This suggests that, despite the improved affinity for yohimbine, the fusion of mouse and human sequence in MHCR2 resulted in some incompatibility, which compromised atipamezole binding.

The majority of the candidate residues changed in MHCR2 reside in the third cytoplasmic loop, a region that has not been directly implicated in the determination of ligand-binding specificity. To evaluate whether the human third loop sequence in MHCR2 was responsible for the high yohimbine affinity of this receptor, we replaced the human third loop sequence in MHCR2 with wild-type mouse sequence. This receptor, MHCR3, represents a mouse Mα_2-10H protein in which only four candidate residues (three in EL_2 and one in TM_5) have been changed to their human counterparts. MHCR3 bound

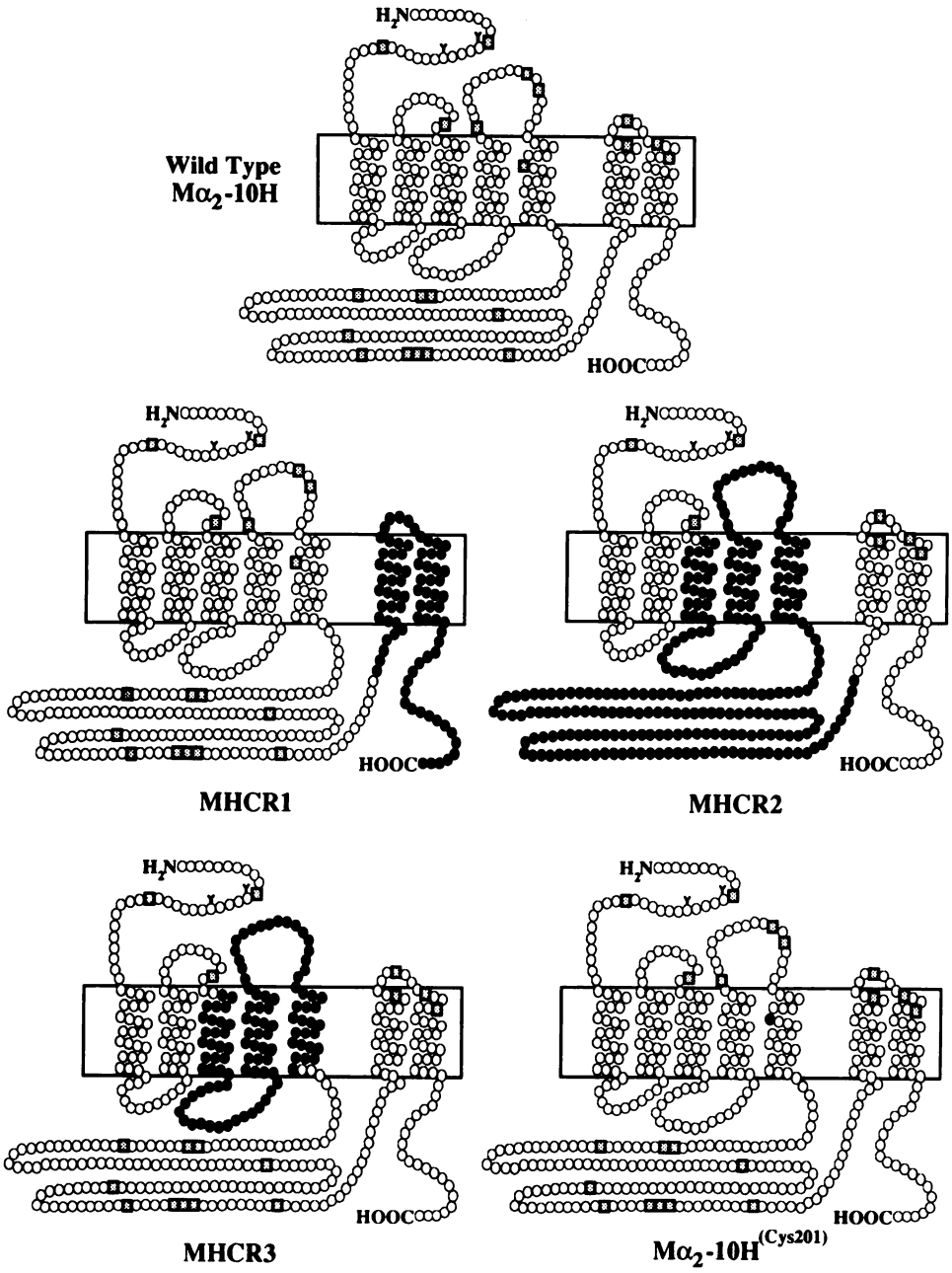

Fig. 6. Model for the structure of wild-type Mα_2-10H and chimeric mouse (Mα_2-10H)/human α_2-C10 receptors. *White circles*, mouse Mα_2-10H sequence; *black circles*, sequence from human α_2-C10; *grey squares*, candidate residues in the mouse sequence potentially responsible for the low affinity of this receptor for yohimbine. These candidate residues are found in both the Mα_2-10H and rat RG20 receptors but are different from residues in these positions in the human α_2-C10 and porcine α_2-C10 homolog (see Results and Fig. 4). The affinities of these chimeric receptors for yohimbine and atipamezole are given in Table 1.

yohimbine (K_d = 4.8 nM) with an affinity almost identical to that of the wild-type human α_2-C10 (K_d = 3.4 nM).

Of the four candidate residues mutated in MHCR3, only one (residue 201) is contained within a transmembrane domain. We surmised, therefore, that this residue was most likely responsible for the high affinity of MHCR3 for yohimbine. To test this possibility, we mutated the serine at this position in Mα_2-10H to a cysteine, the residue found at position 201 in the human α_2-C10. This mutant, Mα_2-10H$^{(Cys^{201})}$, bound yohimbine with an affinity higher than that of the wild-type mouse receptor [Mα_2-10H$^{(Cys^{201})}$, K_d = 10.8 nM; Mα_2-10H, K_i = 53.6 nM] but slightly lower than that of MHCR3 (K_d = 4.8 nM). To facilitate direct comparison, binding assays were performed simultaneously on the mouse Mα_2-10H, the human α_2-C10, and the Mα_2-10H$^{(Cys^{201})}$ point mutant, using the same ligand stocks. A representative [^{3}H]yohimbine competition curve from these experiments is shown in Fig. 7.

Discussion

The cloning and expression of α_2-AR genes from human, rat, and porcine sources have demonstrated that this class of AR is composed of multiple, closely related, subtypes (6–9, 11–13). We have identified and expressed two genes encoding α_2-AR subtypes, the first to be cloned from the mouse genome.

Based on sequence homology and binding data, the mouse Mα_2-4H receptor appears to represent the mouse homolog of the human α_2-C4 subtype (with which it shares 89% homology). The mouse Mα_2-10H receptor exhibits a much higher sequence homology to the human α_2-C10 subtype (92%) than to either the human α_2-C4 (56%) or α_2-C2 (54%). This suggests that Mα_2-10H represents the mouse α_2-C10 homolog. Its pharmacological characterization, however, differs from that of the human α_2-C10, because the mouse Mα_2-10H binds the yohimbine/rauwolscine class of antagonists with significantly lower

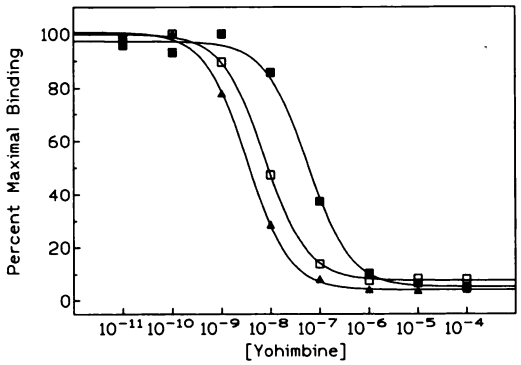

Fig. 7. Representative [^{3}H]yohimbine competition curves for the mouse Mα_2-10H, human α_2-C10, and Mα_2-10H$^{(Cys^{201})}$ point mutant, assayed simultaneously. ■, Wild-type Mα_2-10H; ▲, human α_2-C10; □, the Mα_2-10H$^{(Cys^{201})}$ point mutant. For comparison purposes, binding assays for all three receptors were carried out simultaneously, using the same ligand stocks.

affinity. Another receptor, the rat RG20, also exhibits low yohimbine affinity, despite its high degree of sequence homology to the human α_2-C10. Lanier *et al.* (9) have invoked a new pharmacological class to contain the RG20, the α_2-D, into which the mouse Mα_2-10H receptor would seem to fit.

Because Mα_2-10H diverges from the human α_2-C10 in its pharmacological properties, it is possible that this receptor represents a mouse α_2-AR subtype unique from the α_2-C10 and that another gene exists that encodes the true α_2-C10 homolog. Our Southern blot data do not support this hypothesis, because the 5.1-kb *Pst*I and 9.8-kb *Eco*RI fragments that hybridize most strongly to the human α_2-C10 probe also hybridize to clone Mα_2-10H at high stringency. It appears, therefore, that no other gene exists that has a higher degree of similarity to the human α_2-C10 than does Mα_2-10H. For this reason, we believe that Mα_2-10H represents the mouse homolog of the human α_2-C10 receptor. Differences in binding for the synthetic antagonist yohimbine may simply represent an interspecies variation that has no functional significance *in vivo* and does not justify assignment of the Mα_2-10H as a receptor subtype unique from the α_2-C10. Because the amino acid sequence of RG20 is 96% identical to that of Mα_2-10H and no rat α_2-AR with a higher degree of homology to human α_2-C10 has been cloned, we suspect that the RG20 receptor may represent the rat homolog of human α_2-C10.

The identification of two receptors, the mouse Mα_2-10H and rat RG20, which bind relatively poorly to a single class of α_2-specific antagonist has general implications for the structure of the ligand binding pocket. Both yohimbine and rauwolscine are large, planar, L-shaped molecules composed of interlocked aliphatic rings, features that suggest a rigid structure. In contrast, atipamezole and prazosin lack the L-shape and have potentially more flexible structures. The observation that the Mα_2-10H and RG20 receptors, which bind yohimbine poorly, bind these other antagonists with high affinity suggests three possibilities; either 1) the rodent receptors lack one or more critical residues that interact specifically with yohimbine in human α_2-C10, 2) the rodent receptors have one or more residues that directly sterically inhibit the binding interaction of this large rigid molecule, or 3) yohimbine, due to its inflexibility, is more sensitive than smaller or more flexible antagonists to residue changes in the rodent receptors that result in subtle conformational reorientations within the binding pocket. These subtle changes may be caused by residues far removed from the actual binding pocket.

We have identified 21 candidate residues in the mouse Mα_2-10H receptor that may be involved in the interactions outlined above. These residues are found in both the mouse Mα_2-10H and rat RG20 receptors (yohimbine $K_i > 50$ nM) but are not found in either the human or porcine α_2-C10 receptors (yohimbine $K_d < 10$ nM). By constructing mouse Mα_2-10H/human α_2-C10 chimeric receptors, we have eliminated candidate residues that do not affect yohimbine binding.

The domains involved in determining antagonist binding specificity have been investigated through the construction of chimeric human α_2-C10/human β_2 receptors (25). These studies have shown that the residues that distinguish between β_2-selective and α_2-selective antagonists were found predominantly within the seventh transmembrane domain (25). More recently, a single point mutation in TM_7 (Phe^{412}→Asn) of the human α_2-C10 reduced the binding affinity of yohimbine 350-fold and increased the affinity for alprenolol, a β-selective antagonist, 3000-fold (31). Two candidate residues (Gln^{406} and Asn^{409}) are found in TM_7 of the mouse Mα_2-10H receptor, and another (Pro^{402}) is found at the junction between EL_3 and TM_7. In light of this, we attempted to repair yohimbine and rauwolscine affinity in the mouse Mα_2-10H receptor by replacing these residues with the corresponding residues from TM_7 in the human α_2-C10. Interestingly, MHCR1 (a chimeric Mα_2-10H receptor containing TM_{6-7} from the human α_2-C10) did not show a substantially higher affinity for yohimbine (K_d = 37.0 nM) than did the wild-type mouse receptor (K_i = 53.6 nM). Atipamezole affinity was unchanged (K_d = 1.3 nM). It appears, therefore, that the seventh transmembrane domain does not contain the determinants responsible for reduced yohimbine affinity in the mouse receptor.

A second chimera was constructed (MHCR2), which was composed of mouse Mα_2-10H sequence from the amino terminus to the end of EL_1, human α_2-C10 sequence for TM_3 through the end of CL_3, and mouse Mα_2-10H sequence from TM_6 through the carboxyl terminus. This represents a mouse receptor in which 27 individual residues have been changed to their human counterparts, although only 14 fit the category of candidate residues (three in EL_2, one in TM_5, and nine in CL_3). This receptor bound yohimbine with affinity comparable to that of the wild-type human α_2-C10 (K_d = 8.4 nM). In addition, MHCR2 bound atipamezole with an affinity (K_d = 8.4 nM) more comparable to that of the wild-type human receptor (K_i = 2.9 nM) than the wild-type mouse receptor (K_d = 0.86 nM; 10-fold higher). It appears, therefore, that one or more of these 14 residues are responsible for the unusual antagonist binding properties of the mouse receptor.

Nine of the 14 candidate residues are found in the third cytoplasmic loop, a region that has been implicated in receptor interactions with G proteins but not in antagonist binding specificity (32). Specific differences in this cytoplasmic loop could have general conformational significance, through their effect on the orientation of hydrophobic domains in the membrane. It is possible that yohimbine, due to its size and inflexibility, might be more sensitive to slight reorientations of residues within the ligand-binding pocket than smaller and more flexible ligands such as atipamezole. To investigate the role of candidate residues in the third loop, we constructed a third chimera (MHCR3) by replacing the human third loop

sequence in MHCR2 with the wild-type mouse third loop. MHCR3 contains mouse Mα_2-10H sequence from the amino terminus to the end of EL_1, human α_2-C10 sequence for TM_3 through the end of TM_5, and mouse Mα_2-10H sequence from the start of CL_3 through the carboxyl terminus. As expected, MHCR3 bound yohimbine with an affinity comparable to that of MHCR2 and the wild-type human α_2-C10 (MHCR3, K_d = 4.8 nM; MHCR2, K_d = 8.4 nM; α_2-C10, K_d = 3.4 nM). These results show that residues in the third loop are not responsible for the low yohimbine binding affinity of the mouse Mα_2-10H receptor. In addition, MHCR3 bound yohimbine with higher affinity than did MHCR2, even though MHCR2 contains more human sequence. These results suggest that some form of subtle incompatibility exists between the transplanted human third loop and wild-type mouse sequences present in MHCR2.

MHCR3 represents a mouse Mα_2-10H receptor in which only four residues have been converted to their human counterparts. Three of these residues are found in EL_2. Only one of the four residues, Ser^{201}, is found in a transmembrane domain (TM_5), as defined by Guyer *et al.* (13). Based on the important role of the transmembrane domains in defining the ligand-binding pocket, we considered Ser^{201} as potentially responsible for the low yohimbine affinity of the mouse receptor. A cysteine is found at the corresponding position in the human and porcine α_2-C10 receptors, both of which bind yohimbine with high affinity. To test our hypothesis, we generated a point mutation at position 201 in the mouse Mα_2-10H receptor, converting the serine to a cysteine. This single point mutation resulted in a 5-fold increase in the yohimbine binding affinity for the mouse Mα_2-10H receptor [Mα_2-10H$^{(Cys^{201})}$, K_d = 10.8 nM; wild-type Mα_2-10H, K_i = 53.6 nM]. It is also interesting that the point mutant does not bind yohimbine as well as does MHCR3 (K_d = 4.8 nM). This suggests that the three candidate residues present in the second extracellular loop of the mouse receptor might also play a minor role in conferring a lower yohimbine affinity on this receptor. Perhaps the mouse extracellular loops interact in some way to impede the access of the large yohimbine molecule to the ligand-binding pocket.

A serine for cysteine mutation is considered very conservative, because the two amino acids are similar in molecular size. This residue exchange might block the formation of a disulfide bond, but changes in ligand binding affinity due to such a drastic perturbation in structure would probably not be limited to a single class of antagonists. Serine and cysteine also differ in pK_a, hydrophobicity, and hydrogen bonding characteristics. Yohimbine contains a series of interconnected hydrocarbon rings, which are very hydrophobic. A water molecule hydrogen-bonded to a serine residue might require displacement for yohimbine to enter the binding pocket. In contrast, the hydrophobic side chain of cysteine could interact more favorably with this hydrophobic ligand, translating into a subtle increase in binding affinity for the human receptor. An alternative hypothesis is that yohimbine, due to its large size, must break a hydrogen bond between adjacent transmembrane helices to enter the ligand-binding pocket of the mouse receptor. The hydrogen bonding capacity of the sulfur-containing amino acids (methionine and cysteine) remains unclear (33). It is possible, therefore, that such an obstructive hydrogen bond does not exist at this position in the human receptor. The energy barrier for yohimbine binding might, consequently, be slightly lower, resulting in a higher affinity interaction.

In conclusion, the cloning of two mouse α_2-AR subtypes has confirmed that the subtype diversity observed in humans also exists in mice and that the mouse receptors share subtype-specific structural features with their human homologs. These genomic clones should also serve as valuable reagents for the study of α_2-AR function in transgenic animals. The identification that the mouse Mα_2-10H binds the yohimbine/rauwolscine class of antagonists with lower affinity than does its human homolog (α_2-C10) has general implications for the use of these compounds to study α_2-AR function in mice. Finally, through the construction of chimeric mouse/human α_2-C10 receptors, we have provided evidence that Ser^{201} in the mouse Mα_2-10H is responsible for the low yohimbine binding affinity of this receptor.

Acknowledgments

The authors would like to thank Dr. H. Roelink for the gift of the ES cell genomic library.

References

1. Ruffolo, R. R. J., A. J. Nichols, and J. P. Hieble. Functions mediated by *alpha*-2 adrenergic receptors., in *The Alpha-2 Adrenergic Receptors* (L. E. Limbird, eds.). Humana Press, Clifton, NJ, 187–280 (1988).
2. Segal, I. S., R. G. Vickery, J. K. Walton, V. A. Doze, and M. Maze. Dexmedetomidine diminishes halothane anesthetic requirements in rats through a postsynaptic *alpha*-2 adrenergic receptor. *Anesthesiology* **69**:818–823 (1988).
3. Cotecchia, S., B. K. Kobilka, K. W. Daniel, R. D. Nolan, E. Y. Lapetina, M. G. Caron, R. J. Lefkowitz, and J. W. Regan. Multiple second messenger pathways of *alpha*-adrenergic receptor subtypes expressed in eukaryotic cells. *J. Biol. Chem.* **265**:63–69 (1990).
4. Bylund, D. B., C. Ray-Prenger, and T. J. Murphy. *Alpha*-2A and *alpha*-2B adrenergic receptor subtypes: antagonist binding in tissues and cell lines containing only one subtype. *J. Pharmacol. Exp. Ther.* **245**:600–607 (1988).
5. Bylund, D. B. Subtypes of *alpha*-2 adrenoceptors: pharmacological and molecular biological evidence converge. *Trends Pharmacol. Sci.* **9**:356–361 (1988).
6. Kobilka, B. K., H. Matsui, T. S. Kobilka, F. T. Yang, U. Francke, M. G. Caron, R. J. Lefkowitz, and J. W. Regan. Cloning, sequencing, and expression of the gene coding for the human platelet *alpha*-2-adrenergic receptor. *Science (Washington D. C.)* **238**:650–656 (1987).
7. Regan, J. W., T. S. Kobilka, F. T. Yang, M. G. Caron, R. J. Lefkowitz, and B. K. Kobilka. Cloning and expression of a human kidney cDNA for an *alpha*-2-adrenergic receptor subtype. *Proc. Natl. Acad. Sci. USA* **85**:6301–6305 (1988).
8. Lomasney, J. W., W. Lorenz, L. F. Allen, K. King, J. W. Regan, F. T. Yang, M. G. Caron, and R. J. Lefkowitz. Expansion of the *alpha*-2-adrenergic receptor family: cloning and characterization of a human *alpha*-2-adrenergic receptor subtype, the gene for which is located on chromosome 2. *Proc. Natl. Acad. Sci. USA* **87**:5094–5098 (1990).
9. Lanier, S. M., S. Downing, E. Duzic, and C. J. Homcy. Isolation of rat genomic clones encoding subtypes of the *alpha*-2 adrenergic receptor. *J. Biol. Chem.* **266**:10470–10478 (1991).
10. Voigt, M. M., S. K. McCune, R. Y. Kanterman, and C. C. Felder. The rat *alpha*-2C4 adrenergic receptor gene encodes a novel pharmacological subtype. *FEBS Lett.* **278**:45–50 (1991).
11. Zeng, D. W., J. K. Harrison, D. D. D'Angelo, C. M. Barber, A. L. Tucker, Z. H. Lu, and K. R. Lynch. Molecular characterization of a rat *alpha*-2B-adrenergic receptor. *Proc. Natl. Acad. Sci. USA* **87**:3102–3106 (1990).
12. Chalberg, S. C., T. Duda, J. A. Rhine, and R. K. Sharma. Molecular cloning, sequencing and expression of an *alpha*-2-adrenergic receptor complementary DNA from rat brain. *Mol. Cell. Biochem.* **97**:161–172 (1990).
13. Guyer, C. A., D. A. Horstman, A. L. Wilson, J. D. Clark, E. J. Cragoe, and L. E. Limbird. Cloning, sequencing, and expression of the gene encoding the porcine *alpha*-2-adrenergic receptor: allosteric modulation by Na^+, H^+, and amiloride analogs. *J. Biol. Chem.* **265**:17307–17317 (1990).
14. Lorenz, W., J. W. Lomasney, S. Collins, J. W. Regan, M. G. Caron, and R. J. Lefkowitz. Expression of three α_2-adrenergic receptor subtypes in rat tissues: implications for α_2 receptor classification. *Mol. Pharmacol.* **38**:599–603 (1990).
15. Zeng, D., and K. R. Lynch. Distribution of *alpha*-2-adrenergic receptor mRNAs in the rat CNS. *Mol. Brain Res.* **10**:219–225 (1991).
16. Kurose, H., J. W. Regan, M. G. Caron, and R. J. Lefkowitz. Functional interactions of recombinant *alpha*-2 adrenergic receptor subtypes and G proteins in reconstituted phospholipid vesicles. *Biochemistry* **30**:3335–3341 (1991).
17. Capecchi, M. R. Altering the genome by homologous recombination. *Science (Washington D. C.)* **244**:1288–1292 (1989).
18. Chisaka, O., and M. R. Capecchi. Regionally restricted developmental defects

resulting from targeted disruption of the mouse homeobox gene hox-1.5. *Nature (Lond.)* **350**:473–479 (1991).
19. Soriano, P., C. Montgomery, R. Geske, and A. Bradley. Targeted disruption of the c-*src* proto-oncogene leads to osteopetrosis in mice. *Cell* **64**:693–702 (1991).
20. Sanger, G., S. Nicklen, and A. R. Coulson. DNA sequencing with chain-terminating inhibitors. *Proc. Natl. Acad. Sci. USA* **74**:5463–5467 (1977).
21. Fawcett, T. W., and S. G. Bartlett. An effective method for eliminating "artifact banding" when sequencing double-stranded DNA templates. *Biotechniques* **9**:46–48 (1990).
22. Needleman, S., and C. Wunsch. A general method applicable to the search for similarities in the amino acid sequence of two proteins. *J. Mol. Biol.* **48**:443–453 (1970).
23. Smith, T. F., and Waterman, M. S. Comparison of biosequences. *Adv. Appl. Math.* **2**:482–489 (1981).
24. Cullen, B. Use of eukaryotic expression technology in the functional analysis of cloned genes. *Methods Enzymol.* **152**:684–704 (1987).
25. Kobilka, B. K., T. S. Kobilka, K. Daniel, J. W. Regan, M. G. Caron, and R. J. Lefkowitz. Chimeric *alpha*2-,*beta*2-adrenergic receptors: delineation of domains involved in effector coupling and ligand binding specificity. *Science (Washington D. C.)* **240**:1310–1316 (1988).
26. Kozak, M. The scanning model for translation: an update. *J. Cell Biol.* **108**:229–241 (1989).
27. Dohlman, H. G., M. G. Caron, and R. J. Lefkowitz. A family of receptors coupled to guanine nucleotide regulatory proteins. *Biochemistry* **26**:2657–2664 (1987).
28. Henderson, R., J. M. Baldwin, T. A. Ceska, F. Zemlin, E. Beckmann, and K. H. Downing. Model for the structure of bacteriorhodopsin based on high-resolution electron cryo-microscopy. *J. Mol. Biol.* **213**:899–929 (1990).
29. Walker, J. E., M. Saraste, M. J. Runswick, and N. J. Gay. Distantly related sequences in the α- and β-subunits of ATP synthase, myosin, kinases, and other ATP-requiring enzymes and a common nucleotide binding fold. *EMBO J.* **1**:945–951 (1982).
30. Virtanen, R. Pharmacological profiles of medetomidine and its antagonist, atipamezole. *Acta Vet. Scand.* **85**:29–37 (1989).
31. Suryanarayana, S., D. A. Daunt, M. von Zastrow, and B. K. Kobilka. A point mutation in the seventh hydrophobic domain of the *alpha*-2 adrenergic receptor increases its affinity for a family of *beta* receptor antagonists. *J. Biol. Chem.* **266**:15488–15492 (1991).
32. O'Dowd, B. F., R. J. Lefkowitz, and M. G. Caron. Structure of the adrenergic and related receptors. *Annu. Rev. Neurosci.* **12**:67–83 (1989).
33. Baker, E. N., and R. E. Hubbard. Hydrogen bonding in globular proteins. *Prog. Biophys. Mol. Biol.* **44**:97–179 (1984).

Send reprint requests to: Brian Kobilka, Room B157, Beckman Center, Stanford University, Stanford, CA 94305.